Determination of the IMF on the basis of a recently derived SFR history in the solar neighbourhood

W. J. Maciel* and H. J. Rocha-Pinto

Instituto Astronômico e Geofísico, Av. Miguel Stefano 4200, 04301-904 São Paulo SP, Brazil

ABSTRACT

The initial mass function (IMF) in the solar neighbourhood is determined on the basis of a recently derived history of the star formation rate (SFR) which shows the presence of a star formation burst about 8 Gyr ago. The observed present-day mass function (PDMF) is considered, and the average past distribution of stars of a given mass is estimated. Two cases are considered, namely (i) constant SFR, and (ii) variable SFR as derived from the new metallicity distribution of G dwarfs. The resulting IMF is compared with previous determinations by Scalo and Kroupa et al., and the variation with stellar mass of the slope of the IMF is compared with reference determinations in the literature.

Key words: stars: formation – stars: luminosity function, mass function – Galaxy: evolution – solar neighbourhood.

1 INTRODUCTION

The local initial mass function (IMF) is a basic quantity in the study of the chemical evolution of our Galaxy, as it determines the number of stars formed in a given mass interval in the solar neighbourhood (Tinsley 1980; Scalo 1978, 1986). Recently, a new metallicity distribution of G dwarfs in the solar neighbourhood has been derived by Rocha-Pinto & Maciel (1996), which showed considerable differences relative to the classical distribution by Pagel & Patchett (1975). This led to a new determination of the history of the relative star formation rate (SFR) in the Galaxy (Rocha-Pinto & Maciel 1997), where it was shown that the new results are consistent with the existence of at least one major star formation event, or burst, which occurred about 8 Gyr ago. There may therefore have been appreciable differences in the SFR as compared with a constant history, which is supported by other independent investigations (Majewski 1993).

In this paper we study the effect of the newly derived SFR history on the local IMF, regarding both the high-mass and the low-mass ends of the IMF. We have taken into account the present-day mass function (PDMF) as given by Scalo (1986) and Kroupa, Tout & Gilmore (1993). The differences relative to a constant-SFR history are analysed, and the resulting IMF is compared with previous determinations in the literature.

2 THE IMF AND THE PDMF

We will consider the IMF in the form $\xi(\log m)$, which is given in units of number of stars per logarithmic mass interval per square parcsec (cf. Miller & Scalo 1979; Tinsley 1980; Scalo 1986).

* E-mail: maciel@orion.iagusp.usp.br (WJM)

The determination of the IMF is based on the PDMF, which gives the present number of stars on the main sequence with masses in the interval $(m, m + \mathrm{d}m)$ per square parsec. The relation between the IMF and the PDMF can be found in Tinsley (1980) for stars having lifetimes longer or shorter than the age of the Galaxy, $t_1 = 13$ Gyr, or, equivalently, that have masses lower or shorter than the present turnoff mass, $m < m_1$. According to Tinsley (1980), these relations are valid if the IMF is time-independent, or if $\xi(\log m)$ is interpreted as the *average* past IMF.

Average stellar lifetimes for stars with masses in the range $60 > m > 0.8$ M$_\odot$ are given by Tinsley (1980). An approximation, based on stellar evolutionary models for Population I stars given by Bahcall & Piran (1983), is

$$\log t_m = 10.0 - 3.6 \log m + (\log m)^2, \tag{1}$$

where t_m is given in yr and m in solar masses. According to Bahcall & Piran, typical accuracies for these lifetimes are of the order of 10 per cent, an optimistic result according to Scalo (1986), who suggests uncertainties of about 40 per cent for $m \gtrsim 1.5$ M$_\odot$ and 20 per cent for smaller masses.

The PDMF given by Scalo (1986), $\phi_{\mathrm{ms}}(\log m)$ is defined as the number of main-sequence stars with mass m per unit logarithmic mass interval per pc^2, and is shown in Fig. 1 (crosses). This function has been extrapolated to an upper mass limit $m_\mathrm{u} = 100$ M$_\odot$ and then interpolated in the mass interval $0.1 \le m \le 100$, as shown in Fig. 1 (dotted curve labelled Scalo).

As an alternative PDMF, we have also taken into account the more recent results by Kroupa et al. (1993), which show considerably different results from the Scalo (1986) PDMF, especially at the low-mass end (cf. Kroupa 1998). At the high-mass end, both functions are similar, although the Kroupa et al. (1993) PDMF shows some excess of stars with $m > 2.5$ M$_\odot$ relative to the Scalo
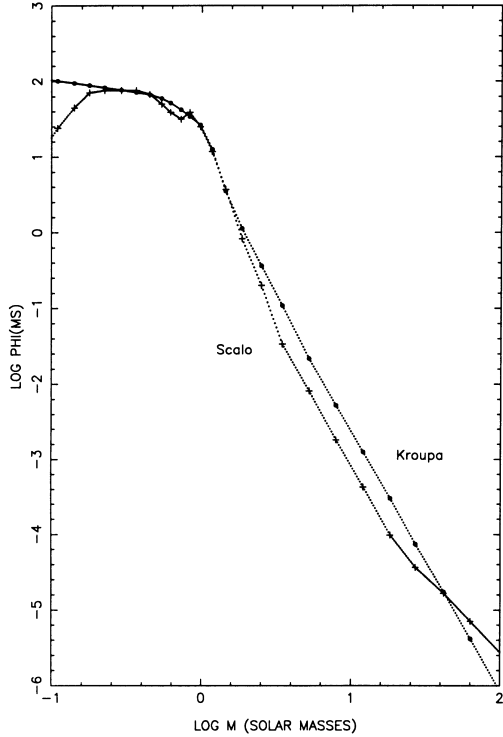
Figure 1. The present-day mass function [stars $\log^{-1} m$ pc^{-2}] as given by Scalo (1986, crosses) and interpolated values (dots). Also shown is the PDMF by Kroupa et al. (1993).

(1986) PDMF. This function is also shown in Fig. 1, where the filled circles refer to the stellar masses in the Scalo (1986) data.

It should be noted that most PDMFÇs found in the literature, such as those shown in Fig. 1, are smoothed functions, generally derived by applying a continuously varying function to the whole mass range. This fact has some important consequences, particularly near $m \simeq 1$ $M_\odot$, where some structures are often found in the PDMF, as shown in the Scalo (1986) PDMF (Fig. 1), or in the PDMF corrected for unresolved multiple stellar systems by Basu & Rana (1992). On the other hand, the average uncertainty of the PDMF near that mass is estimated as 20–30 per cent (cf. Basu & Rana 1992), which corresponds approximately to 0.27 dex, so that the existence of the observed structures is uncertain.

3 THE SFR OF ROCHA-PINTO AND MACIEL

The history of the SFR in the solar neighbourhood was investigated by Rocha-Pinto & Maciel (1997), on the basis of a recently determined metallicity distribution of G dwarfs (Rocha-Pinto & Maciel 1996). The method uses simultaneously the metallicity distribution and the age–metallicity relation, and associates the number of stars in a given metallicity interval with the corresponding time interval predicted by the age–metallicity relation. Corrections are considered to account for observational errors, cosmic scatter and scaleheight effects. The application of the method to the solar neighbourhood shows evidences for at least two events of star formation, namely a burst some 8 Gyr ago and a lull 2–3 Gyr ago, adopting $t_1 = 13$ Gyr.

The history of the relative SFR, $b(t)$, as derived by Rocha-Pinto & Maciel (1997, RPM), is given in column 2 of Table 1 for 1-Gyr bins up to the adopted age of the Galaxy.

The normalization condition as applied to the relative SFR

Table 1. Mean SFR history for the local disc.

t (Gyr)	$b(t)$ (RPM)	$b(t)$ (RPM, mod.)
0–1	1.14	1.14
1–2	0.79	0.79
2–3	1.09	1.26
3–4	1.26	1.43
4–5	1.64	1.81
5–6	1.42	1.59
6–7	1.14	1.31
7–8	0.95	0.95
8–9	0.78	0.78
9–10	0.61	0.61
10–11	0.54	0.54
11–12	0.39	0.39
12–13	1.28	0.39

gives

$$\bar{b}_1 = \frac{1}{t_1} \int_0^{t_1} b(t) dt = 1 \qquad (2)$$

(cf. Miller & Scalo 1979 and Scalo 1986), and we notice that in this case $b(t_1) = \bar{b}_1 = 1.28$. As discussed by Rocha-Pinto & Maciel (1997), this value can be considered as an upper limit, since the growth of the relative SFR at t_1 as observed in Table 1 may be an artificial feature of the method used. It is therefore interesting to consider the case where the SFR has remained essentially constant for the last two bins of Table 1. As suggested by the simulations performed in order to recover the past SFR (cf. Rocha-Pinto & Maciel 1997), we have then assumed the excess SFR in the last bin to be equally distributed through the burst between 2 and 7 Gyr, which corresponds to an additional ratio $\Delta b = 0.17$ in that range. A new SFR history is obtained, which is then a modification of the original SFR by Rocha-Pinto & Maciel (1997). This is given in column 3 of Table 1, and we note that $\bar{b}_1 = 0.39$, which is a convenient lower limit. As we will see in the next section, our results are sensitive to the values of the relative SFR at t_1. In the following, we will denote the obtained limits as $b_1^+ = 1.28$ and $b_1^- = 0.39$ respectively.

## 4 RESULTS AND DISCUSSION

4.1 Constant SFR

Let us initially examine the situation of a constant SFR, which corresponds to $b(t) = 1$. We will present our results as the IMF $\xi(\log m)$, and also the total amount of mass contained in the IMF, or the cumulative mass distribution of the IMF ($M_\odot$ pc^{-2}) given by

$$\mathcal{M} = \int_{m_l}^{m_u} m \, \xi(\log m) d\log m = \log e \int_{m_l}^{m_u} \xi(\log m) dm. \qquad (3)$$

The limits are in practice given by $m_l \simeq 0.1$ $M_\odot$ and $m_u \simeq 100$ $M_\odot$ (cf. Miller & Scalo 1979, equations 38 and 40). In this case, the SFR in the form $\psi(t)$ given in $M_\odot$ pc^{-2} Gyr^{-1} (cf. Tinsley 1980) is related to the relative SFR in the form $b(t)$ by

$$\psi(t) = \frac{b(t)}{t_1} \mathcal{M}. \qquad (4)$$

The IMF $\xi(\log m)$ as a function of the stellar mass is shown in Figs 2(a) and 3(a) for the Scalo (1986) and Kroupa et al. (1993) PDMFs respectively (irregular solid lines). In Fig. 2(a), the crosses represent the IMF as derived by Scalo (1986), and in Fig. 3(a) the asterisks show the corresponding IMF by Kroupa et al. (1993). We can see that for the lower masses ($m < 1$ $M_\odot$), our IMF is essentially the
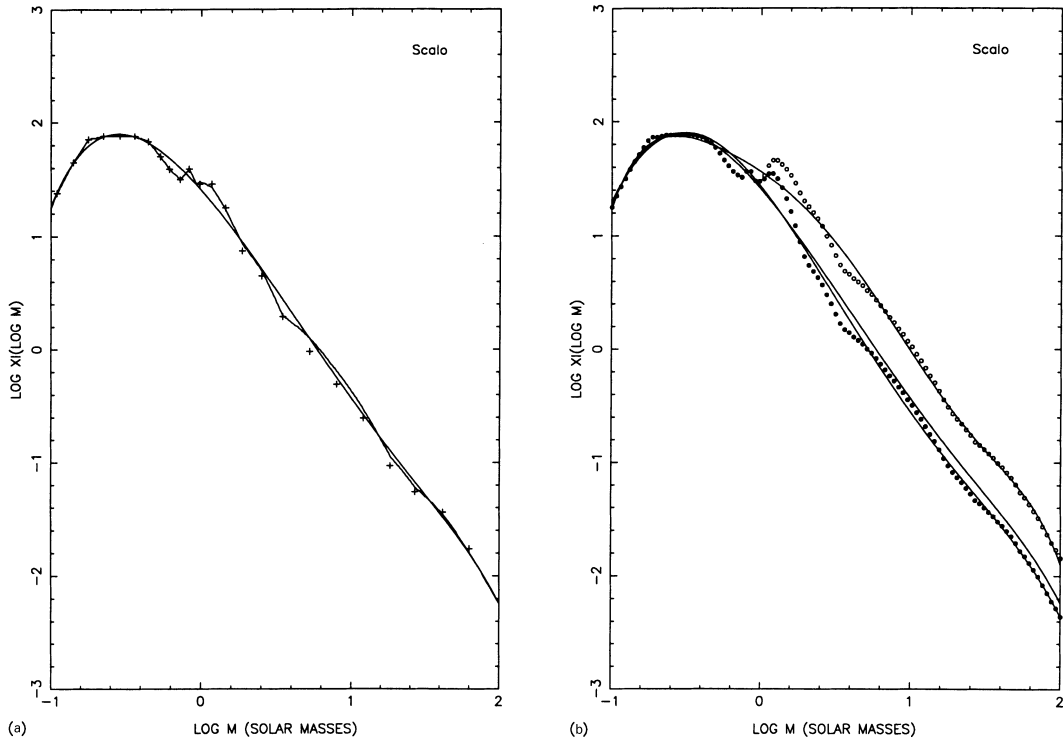
Figure 2. (a) The IMF $\xi(\log m)$ with the PDMF by Scalo (1986) for a constant SFR (irregular solid line). Also shown are a polynomial fit to the IMF and the Scalo IMF (crosses). (b) The same as (a) for a variable SFR with $b_1 = b_1^+$ (filled circles) and $b_1 = b_1^-$ (empty circles), plus the corresponding polynomial fits. Also included is the polynomial fit shown in (a).
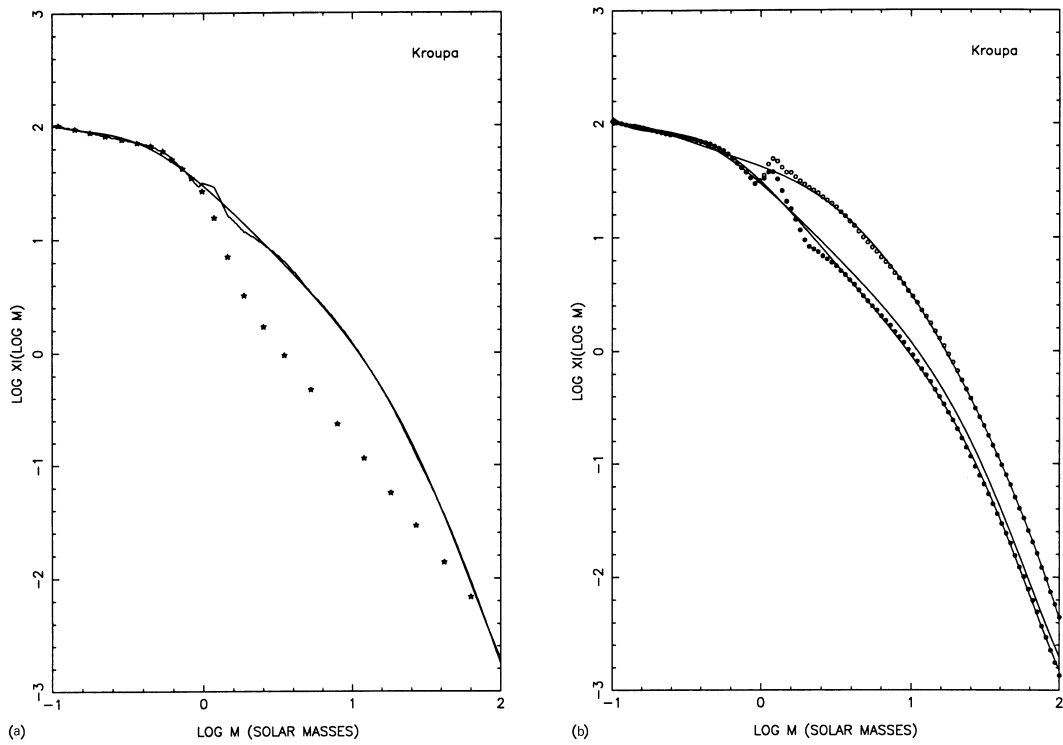
Figure 3. The same as Fig. 2 for the PDMF by Kroupa et al. (1993). The IMF by Kroupa et al. is also shown in panel (a) (asterisks).

Table 2. Cumulative mass and present SFR.

	Scalo	Kroupa et al.
$\mathcal{M}$ (constant SFR)	34.1	47.9
$\mathcal{M}$ (b_1^+)	34.2	45.8
$\mathcal{M}$ (b_1^-)	52.8	82.7
ψ_1 (constant SFR)	2.6	3.7
ψ_1 (b_1^+)	3.4	4.5
ψ_1 (b_1^-)	1.6	2.5

same as the Scalo (1986) IMF (Fig. 2a, crosses), or the Kroupa et al. (1993) IMF (Fig. 3a, asterisks). For the larger masses, our results do not deviate very much from the Scalo IMF, while for the Kroupa et al. (1993) PDMF we obtain a larger number of stars with $m > 2$ M$_\odot$ than implied by their IMF. This discrepancy is essentially due to the different values adopted for the Galactic age and average scale-heights for stars having masses in this mass range.

The cumulative mass $\mathcal{M}$ can be obtained for a constant SFR as a function of the stellar mass for both the Scalo (1986) and the Kroupa et al. (1993) PDMFs. The results are shown in Table 2, where the cumulative mass is given in units of M$_\odot$ pc^{-2}. Analogously, the present SFR ψ_1 can be calculated from equation (4), and is also given in Table 2 in units of M$_\odot$ pc^{-2} Gyr^{-1} for the interval $0.1 - 100$ M$_\odot$. The obtained value can be compared with $\psi_1 = 3.5 - 4.5$ M$_\odot$ pc^{-2} Gyr^{-1} as results from the analytical expressions given by Tinsley (1980), which are derived by Miller & Scalo (1979) for $t_1 = 12$ Gyr using the luminosity function by Wielen (1974). For the Kroupa et al. (1993) PDMF, the cumulative mass and present SFR are also given in Table 2 for the same mass interval. It should be noted that the extrapolation of the Scalo (1986) PDMF from the upper limit $m_u = 63$ M$_\odot$ to $m_u = 100$ M$_\odot$ does not affect the obtained results, as the number of stars near the upper mass limit is expected to be very small.

4.2 Variable SFR

In the case of a variable SFR, the IMF is also time-dependent, and $\xi(\log m)$ is now interpreted as the *average* past IMF derived at $t = t_1$. Again we can determine the IMF taking into account the adopted stellar mass interval. The adopted relative SFR $b(t)$ is the piecewise function given in Table 1 and, as we have seen in Section 3, the relative SFR at t_1 depends on the behaviour of the history of the SFR in the last few bins of Table 1. From our discussion, we can expect the present relative SFR to lie in the range $1.28 \geq b_1 \geq 0.39$. It can be shown that the IMF can then be written as

$$\xi(\log m) = \frac{\alpha}{b_1}\, \xi_0(\log m), \qquad (5)$$

where we have used the subscript '0' for the function $\xi(\log m)$ calculated at a constant SFR. The parameter α is defined as

$$\alpha = \begin{cases} b_1 & (t_m > t_1) \\ 1 & (t_m \ll t_1) \\ \dfrac{b_1}{\dfrac{1}{t_m}\displaystyle\int_{t_1-t_m}^{t_1} b(t)\mathrm{d}t} & (t_m < t_1). \end{cases} \qquad (6)$$

It can be seen from equation (6) that the detailed temporal variations of the SFR $b(t)$ will affect the new $\xi(\log m)$ only for $t_m < t_1$ (excluding $t_m \ll t_1$), which corresponds to a small part of the whole mass range. For objects with $t_m > t_1$ and $t_m \ll t_1$, equation

(6) shows that the piecewise function $b(t)$ of Table 1 does not produce any discontinuities in the IMF.

Therefore, for $t_m > t_1$, we have $\xi(\log m) \simeq \xi_0$, and, at the high-mass extreme, $t_m \ll t_1$ and $\xi(\log m) \simeq \xi_0/b_1$, so that larger differences will appear at large masses. This is shown in Figs 2(b) and 3(b), where the filled circles correspond to $b_1 = b_1^+$, and the empty circles refer to $b_1 = b_1^-$. We see that (i) the IMF in the form $\xi(\log m)$ is essentially unchanged for lower masses, $m \leq 1.0$ M$_\odot$, and $t_m > t_1$; (ii) for higher masses, $m > 1.0$ M$_\odot$, $\xi(\log m)$ increases up to 157 per cent relative to ξ_0 with a peak at $m = 1.2$ M$_\odot$ if the SFR has been constant in the last two bins of Table 1, that is, $b_1 = b_1^-$. Adopting a rising SFR at the last few Gyr, the IMF increases up to 41 per cent for $1.7 > m > 1.0$ M$_\odot$, also with a peak at $m = 1.2$ M$_\odot$, and decreases up to 26 per cent for $m > 1.7$ M$_\odot$. Therefore the presence of the SFR burst detected by Rocha-Pinto and Maciel (1997) affects the IMF in the form $\xi(\log m)$ in different ways, depending on the behaviour of the relative SFR at recent times. If the relative SFR remains essentially constant in the last few Gyr, the presence of the burst implies a higher production of large mass stars. On the other hand, if $b(t)$ is allowed to increase near t_1, the effect of the burst is smoothed, and the IMF does not differ considerably from the reference value ξ_0.

The derived IMF $\xi(\log m)$ can be directly compared with the IMF derived by Scalo (1986) for a constant relative SFR and $t_1 = 12$ Gyr, as shown in Fig. 2(a) (crosses). It can be seen that the Scalo IMF resembles very closely our results both for $b(t) = $ constant (irregular solid line in Fig. 2a), and for $b_1 = b_1^+$ (filled circles in Fig. 2b). For $b_1 = b_1^-$ (empty circles in Fig. 2b), our derived IMF shows an excess of massive stars relative to the Scalo (1986) IMF. The comparison of the IMF with a variable SFR with the results by Kroupa et al. (1993, Fig. 3a, asterisks) shows an even higher over-abundance of high-mass stars, but this can be attributed to different adopted parameters, as mentioned in Section 4.1.

The existence of a burst occurring some τ Gyr ago would result in a ledge in the PDMF near the mass whose main-sequence lifetime is τ (cf. Scalo 1987 and Noh & Scalo 1990). Since the burst detected by Rocha-Pinto & Maciel (1997) occurred between $t \simeq 2$ and $\simeq 7$ Gyr, adopting the lifetimes (equation 1), such a ledge is expected to be broadly located near $m \simeq 1.2$ M$_\odot$. The Scalo (1986) PDMF clearly shows some enhancements near that mass range, but it should be kept in mind that most determinations of the PDMF use a smoothed function, so that one cannot be sure at this stage of the small-scale variations of the IMF at a given stellar mass, as shown for example in Fig. 2(b) for $m = 1.2$ M$_\odot$. Physically, the local maxima on the IMF could have been produced by the burst itself. In fact, near the epoch of the burst, a relatively larger fraction of more massive stars could have been produced, since our approach here is intended to recover the *average* past IMF. However, that is not the only possible explanation, especially in view of the fact that the small structural details on the PDMF are not well known, and may propagate into the derived IMF, as mentioned above. Therefore it seems safer to take a conservative approach, and obtain a smoothed version of our IMF, postponing the determination of the detailed behaviour of this function until the PDMF is more accurately known. This is also done in Figs 2(b) and 3(b), where the IMF for a rising SFR at $t = t_1$ (filled circles) and for a constant SFR at $t = t_1$ (empty circles) are shown along with sixth-order polynomials of the form

$$\log \xi(\log m) = \sum_{n=0}^{6} a_n (\log m)^n, \qquad (7)$$

where the coefficients are given in Table 3 for both the Scalo (1986)

Table 3. Coefficients of the polynomial fits to the IMF (S: Scalo PDMF, K: Kroupa et al. PDMF).

| n	$a_n(b_1^+)$ (S)	$a_n(b_1^-)$ (S)	$a_n(b_1^+)$ (K)	$a_n(b_1^-)$ (K)
0	1.426796	1.557462	1.489590	1.620256
1	−1.636004	−0.879337	1.489590	1.620256
2	−0.993780	−0.574181	−0.676451	−0.256852
3	0.750025	−0.311909	0.635773	−0.426161
4	−0.055413	−0.186031	0.062515	−0.068104
5	−0.046449	0.562851	−0.422926	0.186374
6	0.002651	−0.186622	0.130674	−0.053297

(S) and Kroupa et al. (1993) (K) PDMFs respectively. For comparison purposes, we have also included in Figs 2(b) and 3(b) the polynomial fits corresponding to a constant SFR, already shown in Figs 2(a) and 3(a) (smooth solid lines). It can be seen from Figs 2(b) and 3(b) that the main conclusions regarding the effects of the variable SFR remain valid, in particular the higher production of high-mass stars as compared with a constant SFR. This is clearly a more robust result, as it does not depend on the uncertain structures on the IMF as shown by the filled/empty circle curves on these figures.

Although we did not attempt to derive a power-law IMF, it is interesting to compare the slopes of the derived IMF with reference slopes from the literature. From the IMF by Salpeter (1955), we have $\Gamma = -1.35$, and from the analytical IMF given by Tinsley (1980) on the basis of the Miller & Scalo (1979) IMF we have

$$
\begin{aligned}
\Gamma &= -0.25 & (0.1 < m \leq 1.0) \\
&= -1.00 & (1.0 < m \leq 2.0) \\
&= -1.30 & (2.0 < m \leq 10.0) \\
&= -2.30 & (m > 10.0).
\end{aligned} \tag{8}
$$

More recently, Padoan, Nordlund & Jones (1997) derived new slopes on the basis of numerical experiments of supersonic random flows in molecular clouds. Results for a typical molecular cloud with temperature $T = 10$ K, mean density $n = 1000$ cm^{-3}, and velocity dispersion $\sigma_v = 2.5$ km s^{-1}, range from $\Gamma \simeq 1$ for $m \simeq 0.1$ M$_\odot$ to $\Gamma \simeq -3$ for $m \simeq 10$ M$_\odot$.

These values can be easily compared with our results, adopting the polynomial fits (equation 7) of the IMF. It can be concluded that the slopes for $b_1 = b_1^+$ do not change more than about 10–16 per cent for $6 > m/\text{M}_\odot > 1$ relatively to a constant-SFR slope, which agrees very closely with the slopes by Scalo (1986), as expected, since the IMF does not differ very much from the constant-SFR result. For $b_1 = b_1^-$, the slopes increase up to 85–120 per cent for $5 > m > 0.4$ M$_\odot$, and are closer to the Miller & Scalo (1979) slopes in that range. A good agreement is also obtained with the slopes by Padoan et al. (1997), particularly in the range $-0.7 \leq \log m \leq 0.6$. Adopting the Kroupa et al. (1993) PDMF, the slopes are closer to the Miller & Scalo result, especially for the lowest masses. For masses higher than about one solar mass, our slopes are similar or somewhat steeper than the Salpeter (1955) slope, with some flattening for lower masses, especially for the Kroupa et al. (1993) PDMF. Such behaviour seems to be an ubiquitous feature of the IMF, and can be observed not only for the solar neighbourhood but also for stellar clusters, the Magellanic Clouds and external galaxies (cf. Rana & Basu 1992, Richtler 1994 and Kennicutt 1998). The IMF derived by Rana & Basu was also based on a variable SFR, and takes into account the multiplicity of stars in the solar neighbourhood (Basu & Rana 1992). Their general slopes are steeper than the Salpeter slope for higher masses,
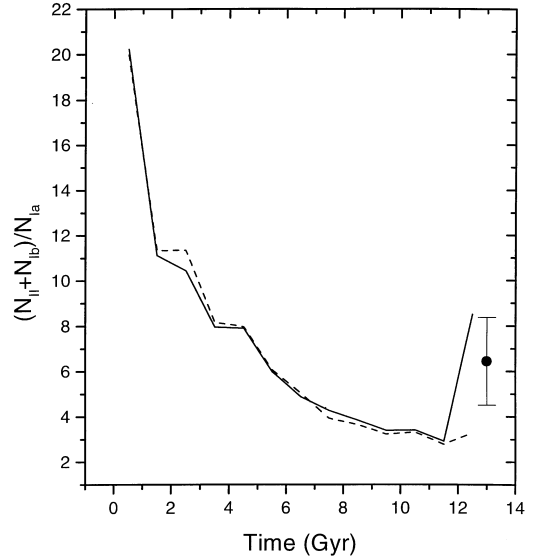
Figure 4. Relative rates for supernovae of types II+Ib and Ia for $b_1 = b_1^+$ (solid line) and $b_1 = b_1^-$ (broken line). The point with error bars shows the observed value.

with some flattening for $m < 1$ M$_\odot$. They have also fitted a polynomial to the IMF instead of a log-normal curve, and their resulting IMF is similar to our result for the Scalo (1986) PDMF shown in Fig. 2(b) with $b_1 = b_1^-$, especially at the higher masses. Also regarding the high-mass end, it is interesting to note that our average slopes do not differ very much from the constant slope $\Gamma \simeq -1.7$ of Kroupa et al. (1993) and Kroupa (1998). In fact, as discussed by Tsujimoto et al. (1997) and Kroupa (1998), there are some evidences for slopes steeper than this value for masses $m > 1 \, rm M_\odot$. Also, our derived slopes are similar to the slopes of the universal IMF discussed by Kennicutt (1998), especially if the Kroupa et al. PDMF is adopted at the low-mass end.

The results for the cumulative mass $\mathcal{M}$ at a variable SFR are also shown in Table 2. Since the cumulative mass depends on $\xi(\log m)$, it can be seen that for a *rising* relative SFR near t_1 the cumulative mass will not differ very much from the constant-SFR value, since the IMFs are very similar, as seen in Figs 2(a) and 3(a). For a *constant* relative SFR near t_1, a larger number of massive stars would form near the epoch of the burst, and the increase in $\xi(\log m)$ at higher masses implies an increase in the cumulative mass up to 55 per cent, as shown in Table 2. With the new cumulative mass, the present rate ψ_1 can be determined, and is also shown in Table 2. It can be seen that, in the case of a rising SFR near t_1, the rate ψ_1 increases by 22–31 per cent, while for a constant SFR near t_1, ψ_1 decreases by 32–38 per cent.

According to the discussion by Rana & Basu (1992), the total surface mass density of the disc obtained from the IMF is in good agreement with the dynamical mass as estimated by Gould (1990) and Kuijken & Gilmore (1991), which is about 50 M$_\odot$pc^{-2} within an estimated uncertainty of about 30 per cent. Taking into account the mass density due to the contributions from evolved stars (0.11 M$_\odot$ pc^{-2}), stellar remnants (3.9 M$_\odot$ pc^{-2}), and gas in the solar neighbourhood (6.6 M$_\odot$ pc^{-2}) as in Rana & Basu (1992), apart from the mass density implied in the PDMF itself (22.0 M$_\odot$ pc^{-2} for the Scalo PDMF, and 25.5 M$_\odot$ pc^{-2} for the Kroupa et al. PDMF), we obtain a total cumulative mass of 32.6 and 36.1 M$_\odot$ pc^{-2} respectively. It can be seen that for the Scalo (1986) PDMF our IMF implies a cumulative mass within the uncertainties,

while for the Kroupa et al. (1993) PDMF the agreement is also good, except for $b_1 = b_1^-$, for which the total mass seems to be in excess of the dynamical mass by approximately 18 $M_\odot$ pc^{-2}.

In view of the results discussed above, it can be concluded that the present relative SFR lies between the limits b_1^+ and b_1^-. A possible way to discriminate between these extremes would involve estimates of the relative frequency of supernovae (SNe) of types II and I. Adopting the expressions for the SN rates as given by Matteucci & Greggio (1986) and the IMFs derived from the Scalo (1986) PDMF, we can determine the SN ratio $N_{II} + N_{Ib}/N_{Ia}$ as a function of time, as shown in Fig. 4. In this figure the solid line represents the case where $b_1 = b_1^+$, and the broken line refers to the case $b_1 = b_1^-$. The point with error bars shows the average observed ratio, $N_{II} + N_{Ib}/N_{Ia} \simeq 6.4 \pm 1.9$ for galaxies with Hubble types between Sb and Sc, as given by van den Bergh & Tammann (1991). Although the observational uncertainties are large, the figure clearly shows that our main conclusions on the SFR are supported, and the present value of the relative SFR value is approximately halfway between the derived limits.

ACKNOWLEDGMENTS

REFERENCES

Bahcall J. N., Piran T., 1983, ApJ, 267, L77

Basu S., Rana N. C., 1992, ApJ, 393, 373
Gould A., 1990, MNRAS, 244, 25
Kennicutt R., 1998, in Howell D. J., Gilmore G. F., Parry I. P. eds, ASP Conf. Ser. Vol. 142, 38th Herstmonceux Conference. in press
Kroupa P., Tout C. A., Gilmore G., 1993, MNRAS, 262, 545
Kroupa P., 1998, in Rebolo R., Martin E. L., Zapatero Osorio M. R. eds, ASP Conf. Ser. Vol. 134, Brown Dwarfs and Extrasolar Planets
Kuijken K., Gilmore G., 1991, ApJ, 367, L9
Majewski S. R., 1993, ARA&A, 31, 575
Matteucci F., Greggio L., 1986, A&A, 154, 279
Miller G. E., Scalo J. M., 1979, ApJS, 41, 513
Noh H. R., Scalo J. M., 1990, ApJ, 352, 605
Padoan P., Nordlund A. P., Jones B. J. T., 1997, MNRAS, 288, 145
Pagel B. E. J., Patchett B. E., 1975, MNRAS, 172, 13
Rana N. C., Basu S., 1992, A&A, 265, 499
Richtler T., 1994, A&A, 287, 517
Rocha-Pinto H. J., Maciel W. J., 1996, MNRAS, 279, 447
Rocha-Pinto H. J., Maciel W. J., 1997, MNRAS, 289, 882
Salpeter E. E., 1955, ApJ, 121, 161
Scalo J. M., 1978, in Gehrels T., ed., Protostars and Planets. Univ. Arizona, p. 265
Scalo J. M., 1986, Fundam. Cosmic Phys., 11, 1
Scalo J. M., 1987, in Thuan T. X., Montmerle T., Van J. T. T., eds, Starbursts and Galaxy Evolution, Editions Frontières, Gif sur Yvette, p. 445
Tinsley B. M., 1980, Fundam. Cosmic Phys., 5, 287
Tsujimoto T., Yoshii Y., Nomoto K., Matteucci F., Thielemann F. K., Hashimoto M., 1997, ApJ, 483, 228
van den Bergh S., Tammann G. A., 1991, ARA&A, 29, 363
Wielen R., 1974, in Contopoulos G., ed., Highlights of Astronomy. Reidel, Dordrecht p. 395

This paper has been typeset from a T$_E$X/L^{A}T$_E$X file prepared by the author.